Sains Malaysiana 55(2)(2026): 257-270
http://doi.org/10.17576/jsm-2026-5502-06

Quaternized Ionic Poly(2-(dimethylamino)ethyl methacrylate) Exhibiting Chain Length and Amphiphilicity Dependent Thermal and Enzymatic Degradation

(Poli(2-(dimetilamino)etil metakrilat) Ion Terkuaternisasi yang Menunjukkan Degradasi Terma dan Enzim Bergantung pada Panjang Rantai dan Amfifilisiti)

NORAFIZAH AHMAD SHAYUTI[1], AINA AQILA ARMAN ALIM[2], SITI FATAHIYAH MOHAMAD[5], NORAZIAH MOHAMAD ZIN[3], NUR HAZLIN HAZRIN-CHONG[4] & RUSLI DAIK[1,*]

[1]*Department of Chemical Sciences, Faculty of Science and Technology, Universiti Kebangsaan Malaysia, 43600 UKM Bangi, Selangor, Malaysia*
[2]*Fuel Cell Institute, Universiti Kebangsaan Malaysia, 43600 UKM Bangi, Selangor, Malaysia*
[3]*Center of Diagnostics, Therapeutics & Investigations, Faculty of Health Sciences, Universiti Kebangsaan Malaysia, Jalan Raja Muda Abdul Aziz, 50300 Kuala Lumpur, Malaysia*
[4]*Department of Biological Sciences and Biotechnology, Faculty of Science and Technology, Universiti Kebangsaan Malaysia, 43600 UKM Bangi, Selangor, Malaysia*
[5]*Radiation Processing and Technology Division, Malaysia Nuclear Agency, 43000 Bangi, Selangor, Malaysia*

Received: 25 September 2025/Accepted: 4 February 2026

ABSTRACT

Amphiphilic polymers derived from quaternized 2-(N, N-dimethylamino)ethyl methacrylate (DMAEMA) were synthesized via radical polymerization to achieve a balance between hydrophilic and hydrophobic segments for antibacterial applications. Quaternization with bromoalkane compounds introduced alkyl side chains, thereby enhancing amphiphilicity and enabling tunable physicochemical properties. The polymers obtained exhibited molecular weights ranging from 1600 to 50600 Da, providing a wide distribution suitable for correlating chain length with performance characteristics. Thermogravimetric analysis confirmed that all samples maintained stability up to 400 °C, indicating robust thermal resistance. Enzymatic degradation studies demonstrated time-dependent surface erosion, with pore formation observed on polymer surfaces beginning at day 5, accompanied by progressive weight reduction. Structural and morphological analyses were performed using Fourier-transform infrared spectroscopy (FTIR), which verified successful functional group modification; meanwhile, scanning electron microscopy (SEM) showed distinct topographical changes associated with amphiphilic behavior and biodegradability of the polymer. Collectively, the findings highlight the successful design of amphiphilic DMAEMA-based polymers with promising thermal stability, controlled degradability, and structural versatility, underscoring their potential utility in antibacterial material development.

Keywords: Amphiphilic polymer; biodegradability; thermal behavior

ABSTRAK

Polimer amfifilik yang diperoleh daripada kuaternisasi 2-(N, N-dimethylamino)etil metakrilat (DMAEMA) telah disintesis melalui pempolimeran radikal yang bertujuan untuk mencapai keseimbangan antara segmen hidrofilik dan hidrofobik sebagai aplikasi antibakteria. Kuaternisasi dengan sebatian bromoalkana dengan penambahan rantai sisi alkil dapat meningkatkan polimer amfifilik dan membolehkan sifat fizikokimia yang boleh dilaras. Polimer yang diperoleh menunjukkan berat molekul antara 1600 hingga 50600 Da, memberikan taburan luas yang sesuai untuk mengaitkan panjang rantai dengan ciri prestasi. Analisis termogravimetri mengesahkan bahawa semua sampel mengekalkan kestabilan sehingga suhu 400 °C, menunjukkan rintangan haba yang baik. Kajian degradasi berenzim menunjukkan hakisan permukaan polimer, dengan pembentukan liang diperhatikan pada permukaan polimer bermula pada hari ke-5, disertai dengan pengurangan jisim polimer yang progresif. Analisis struktur dan morfologi telah dilakukan menggunakan spektroskopi inframerah transformasi Fourier (FTIR) yang mengesahkan pengubahsuaian kumpulan berfungsi telah berjaya manakala mikroskop elektron pengimbasan (SEM) menunjukkan perubahan topografi berbeza yang dikaitkan dengan sifat amfifilik dan kebolehuraian polimer. Secara keseluruhan, kajian ini berjaya mereka bentuk polimer berasaskan DMAEMA dengan sifat amfifilik dengan kestabilan haba yang baik, penguraian terkawal dan kepelbagaian struktur, menggariskan potensi utilitinya dalam pembangunan bahan antibakteria.

Kata kunci: Kebolehuraian; polimer amfifilik; tingkah laku haba

INTRODUCTION

The processes of nature, chemistry, and biology all have an impact on the degradation of amphiphilic polymers, as do circumstances outside, including temperature, sunlight, pH, and the level of humidity (Gaytán, Burelo & Loza-Tavera 2021). Added to that, polymer-specific features such as molecular weight, stereochemistry, crystallinity, and hydrophobic and hydrophilic interactions are breakdown factors (Kupczak, Mielanczyk & Neugebauer 2021a). Poly(2-(dimethylamino)ethyl methacrylate) (DMAEMA) is a multifunctional polymer that has attracted significant attention for applications in antimicrobial, drug delivery carriers, and biofunctional membranes due to its tunable cationic charge density, pH-responsive and amphiphilic nature (Mushtaq et al. 2021; Stawski 2023). Quaternization of poly DMAEMA with alkyl halides, particularly bromoalkanes, produces a quaternized polymer with a permanent cationic charge (Manouras et al. 2021). The length of the alkyl chain introduced during quaternization not only modulates the hydrophilic–hydrophobic balance of the polymer but also alters its degradation behavior under thermal and enzymatic conditions (Li et al. 2018).

Multiple factors, including polymer backbone chemistry, accessibility of hydrolyzable groups, crystallinity, and surface hydrophilicity, govern enzymatic degradation (Aina Aqila, Siti Salwa & Farah Hannan 2022). Enzymes such as lipases and esterases recognize ester linkages in methacrylate-based polymers, catalyzing their cleavage under mild physiological conditions. Surface wettability significantly affects enzyme–polymer interactions: hydrophilic surfaces promote water uptake and enzyme adsorption, while amphiphilic structures can enhance interfacial recognition by lipases, which naturally act at hydrophobic–hydrophilic boundaries (Rahman et al. 2021). In terms of molecular weight, high-molecular-weight polymers resist enzymatic cleavage due to steric hindrance and entanglement, whereas oligomeric or lower-molecular-weight chains undergo more rapid degradation (Im et al. 2023).

In addition, thermal degradation of polymers is primarily dictated by the stability of chemical bonds and the supramolecular organization (crystalline vs amorphous packing, entanglement, hydrogen bonding) of the material. The bond dissociation energy of the polymer backbone and side groups determines the onset of degradation. For instance, polymers containing an ester group often undergo random chain scission, side-group elimination, or depolymerization pathways under heat (Aina Aqila et al. 2023). Molecular weight also plays a significant role in determining which low-molecular-weight polymers degrade at lower temperatures due to reduced chain entanglement and weaker van der Waals forces between shorter chains. Meanwhile, high-molecular-weight polymers require more energy to overcome intermolecular forces and initiate scission (Kong et al. 2021). In case of amphiphilicity, increased hydrophobicity from long alkyl substituents can raise the onset temperature of thermal degradation due to stronger van der Waals interactions, while more hydrophilic parts are prone to earlier decomposition at lower temperature, as it promotes the bond cleavage and destabilizes the polymer structure (Koufakis et al. 2020).

The widespread application of antimicrobial peptides (AMPs) in biomedical and industrial fields is limited by their inherent drawbacks, including high production cost, susceptibility to enzymatic degradation, and potential cytotoxicity (Ali et al. 2025). As a result, there is a growing need for synthetic alternatives that can mimic the antimicrobial activity of AMPs while offering greater stability and cost-effectiveness. Quaternized polymers based on DMAEMA have emerged as promising synthetic mimics of AMPs due to their tunable cationic charge density and amphiphilic balance (Santoro & Izzo 2024). Quaternization using bromoalkanes is particularly advantageous, as the alkylation process not only introduces permanent positive charges that enhance antimicrobial activity but also allows systematic variation of alkyl chain length, thereby modulating amphiphilicity, hydrophobic interactions, and degradation behavior (Koutsougera et al. 2025). This strategy provides a controllable pathway to design stable, cost-effective, and efficient antimicrobial materials that can potentially replace natural AMPs.

Therefore, the objective of this study was to elucidate the relationship between the chain length of bromoalkane quaternization and the amphiphilic structure on the degradation behavior of quaternized DMAEMA-based polymers under thermal and enzymatic conditions, aiming to achieve a balance between hydrophilic and hydrophobic segments for antibacterial applications. The performance of amphiphilic polymers, specifically poly DMAEMA-OB (1-bromooctane) and poly DMAEMA-HdB (1-bromohexadecane) were compared and discussed in terms of molecular weight, phase morphology, thermal behavior and biodegradability.

MATERIALS AND METHODS

2-(N,N-dimethylamino)ethyl methacrylate (DMAEMA) was purified by passing it through a short column of neutral alumina to remove the inhibitors; it was purchased from Acros Organics, 1-bromooctane (OB) and 1-bromohexadecane (HdB) were purchased from Acros Organics. Potassium persulfate (KPS), acetone and chloroform were supplied by Sigma-Aldrich.

SYNTHESIS OF AMPHIPHILIC POLYMER

DMAEMA and a bromoalkane liquid were reacted in ethanol at 60 °C for 24 h to develop the monomer. Each of the monomers (1-bromooctane and 1-bromohexadecane) was subsequently transferred to a 250 mL round-bottom flask with a freshly cleaned and dried closure apparatus

containing a magnetic stirring bar. After approximately ten minutes of vacuuming, the vessel retaining the monomer was purged with nitrogen to eliminate any residual oxygen. Nitrogen gas was introduced into a 0.25 M potassium persulfate (KPS) solution in a separate flask and left for ten minutes. While ensuring there was no vacuum leaking, the KPS solution was carefully transferred into the flask holding the monomer. After that, the mixture was then heated for four hours at 70 °C while submerged in silicone oil.

To cease the reaction, the resultant white liquid is subsequently poured into an enormous amount of acetone. The creation of a white precipitate induces agglomeration. Post filtration, the resultant long-chain polymer was twice cleaned using a 1:1 acetone:water mixture (Lu, Wu & Fu 2007). When it comes to the short-chain polymer, the resulting substance was immersed in chloroform, allowed to clump together, and then filtered through water. After that, the sticky and wet components were left in a vacuum oven for 48 h. The material collected was a brittle, dry solid. Figure 1 shows the reaction involved in the synthesis of both monomer and polymer.

MOLECULAR WEIGHT DETERMINATION

The intrinsic viscosity [ŋ] method was used to determine the molecular weight of the resulting polymer. The temperature of the water immersion was kept at room temperature and monitored throughout the experiment to ensure uniformity. Each polymer was dissolved in ethanol at various concentrations of 2, 5, 10, 15, and 20 mg/mL. The polymer solutions in ethanol were filtered using a 0.45 µm pore-size PTFE syringe filter.

The Ostwald viscometer was then filled with the solution, and the duration of each solution flow was recorded. The Mark-Houwink-Sakurada equation, such as Equation (1), is used to compute the intrinsic viscosity [ŋ].

$$[\eta] = KM_{\eta}^{\alpha} \quad (1)$$

Source: Rauschkolb et al. 2022

where K and M are empirical constants that are directly proportional to the solvent and the temperature used.

POLYMER ENZYMATIC BIODEGRADATION

Lipase was dissolved in phosphate-buffered saline (PBS) to make a buffer-enzymatic solution with a concentration of 1 mg/mL. Biodegradation tests were carried out in a shaker incubator at 37 °C and 150 rpm. Following that, the necessary amount of amphiphilic polymer and enzyme was added to the PBS solution, which was then incubated for several days.

This mixture of reactions was centrifuged for 20 min at 90 °C to denature the enzyme after the procedure. Following the rinsing and drying in pure water, the material was weighed and examined using Fourier-transform infrared (FTIR) and Scanning Electron Microscopy (SEM).

FOURIER-TRANSFORM INFRARED (FTIR) SPECTROSCOPY

The functional groups in the degraded samples were identified using Fourier-transform infrared (FTIR) spectroscopy, with absorbencies that range from 650 to 4000 cm^{-1} at room temperature. Pieces of the samples were placed on the sample holder and the obtained data were interpreted to determine the functional groups in the sample.

SCANNING ELECTRON MICROSCOPY (SEM)

The morphology of the degraded samples on their pore surfaces (after enzymatic hydrolysis) was evaluated using the ZEISS scanning electron microscope (SEM) LEO 1450VP model. To safeguard against electrical discharge,

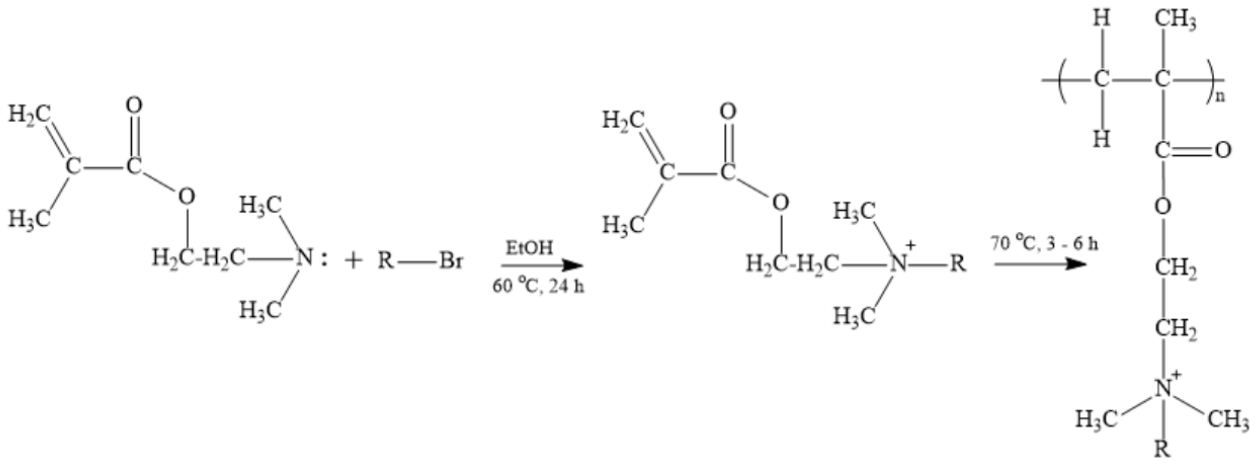

FIGURE 1. Reaction scheme of the synthesis of quaternized monomer and amphiphilic polymer from DMAEMA

the samples were gold-sputtered before viewing. The specimens with coatings were mounted to the sample holders using carbon conductive tape that was secured to the axial steering table of the SEM apparatus. Samples were captured with a 10 kV acceleration voltage.

THERMOGRAVIMETRIC ANALYSIS (TGA)

A NETZSCH STA 449 F3 Jupiter Simultaneous Thermal Analysis (STA) was used to characterize the thermogravimetric analysis and identify the initial and maximum decomposition temperature of the generated polymers. The study used temperatures ranging from 25 to 600 °C and a heating rate of 5 °C/min. A sample containing 15 mg of the synthesized polymers was heated in the sample pan using an environment of nitrogen gas flowing at a rate of 50 mL/min.

RESULTS AND DISCUSSIONS

Amphiphilic polymers, specifically poly DMAEMA-OB and poly DMAEMA-HdB were successfully synthesized via free-radical polymerization. Despite being a white solid, the short-chain amphiphilic polymer (poly DMAEMA-OB) melted readily at ambient temperature. The long-chain amphiphilic polymer (poly DMAEMA-HdB) produced a whitish and brittle solid. The percentage yield of these polymers are 77.7% for poly DMAEMA-OB and 63.8% for poly DMAEMA-HdB. Compared with pure DMAEMA, the polymers with long hydrophobic chains exhibited greater amphiphilicity.

MOLECULAR WEIGHT

The rapid and simple intrinsic viscosity method (Danielsen et al. 2021) was used to find the molecular weight of the amphiphilic polymers. As observed in diluted polymer solutions, the linear relationship between the molecular weight and the intrinsic viscosity can be used to calculate the average molecular weight of the polymers (Rauschkolb et al. 2022). The molecular weight of each polymer was calculated using the Mark-Houwink-Sakurada calculation via intrinsic viscosity determination. It was shown that the molecular weight of the polymers varies with reaction time. The results obtained are summarised in Figure 2.

The molecular weights obtained for all polymers ranged from 1600 Da (poly DMAEMA-HdB) to 50600 Da (poly DMAEMA-OB). These results demonstrate that longer alkyl chain moieties inhibit the formation of polymers with a higher degree of polymerization. The steric hindrance of the macromolecule (Ren, Yu & Zhu 2021) may affect the kinetics of the polymerization reaction (Zografos et al. 2021). In addition, one of the factors causing the significant variation in the molecular weight of these polymers is that the monomer contains a vinyl group, i.e., a highly active electron-pulling group away from the quaternary ammonium positive charge (Fu et al. 2022). In addition, the vinyl group encountered a substantially greater steric hindrance due to the size of the molecule (Bednarz et al. 2014), causing the polymerization reaction to be interrupted.

ENZYMATIC BIODEGRADATION

One well-established method for comprehending the process of decomposition activity is enzyme-based degradation. According to their chemical structures, the lipase enzyme was chosen since each of the amphiphilic polymers produced had an ester group from the DMAEMA backbone. It was discovered that lipase enzymes had favorable ester fission activity characteristics at the hydrophilic-hydrophobic interface (Bixenmann, Stickdorn & Nuhn 2020). The lipase enzyme has the plus point of being water-soluble, yet it is capable of interacting with

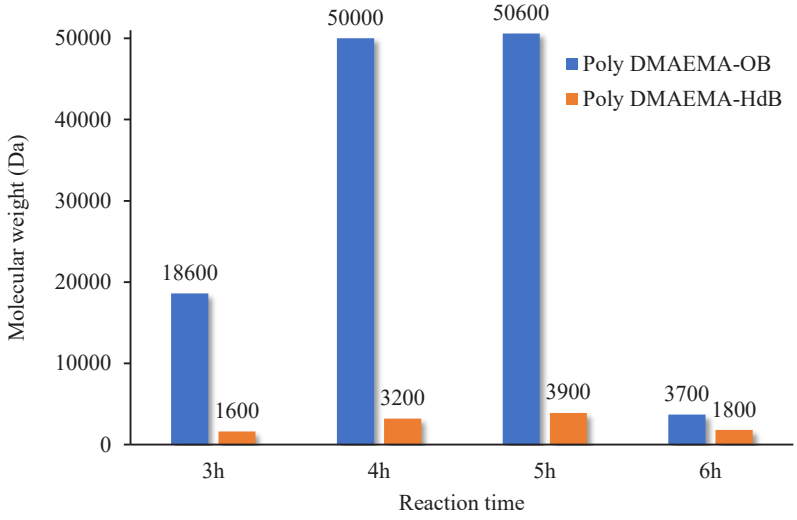

FIGURE 2. Molecular weight of amphiphilic polymers

insoluble substrates to produce an enzyme-substrate complex (E-S) (Albayati et al. 2020; Rodríguez-Contreras, Calafell-Monfort & Marqués-Calvo 2012). This could help degrade water-insoluble poly DMAEMA-HdB.

In this test, a solution of PBS with a pH of 7.4 works well since a solution with an acidic pH will trigger the NH_4^+ cation group, which will cause them to repel one another (Cazotti et al. 2020; Luo et al. 2021). Its enhanced hydrophilic features will make it more vulnerable to hydrolytic breakdown (Kupczak, Mielanczyk & Neugebauer 2021a). Two samples were analyzed in this test, namely poly DMAEMA-OB-5h and poly DMAEMA-HdB-5h. Both samples possess the highest molecular weight, at 3900 Da (poly DMAEMA-OB-5h) and 50600 Da (poly DMAEMA-HdB-5h).

As indicated in Figure 3, each sample demonstrated an increase in percentage weight loss in accordance with an increase in the degradation time period for 21 days. As reported in previous findings by several research groups (Bixenmann, Stickdorn & Nuhn 2020; Casanova et al. 2023; Cook-Chennault et al. 2024; Leggieri et al. 2023), these studies concluded that DMAEMA structures with ester groups are resistant to degradation, which is why the enzymatic hydrolysis reaction takes more than ten days (Cook-Chennault et al. 2024). A negative control test (without lipase enzyme) was utilized as a reference. Both negative control tests resulted in a lower weight loss as compared to the samples with the presence of enzymes. About 50.6% (poly DMAEMA-OB) and 27.7% (poly DMAEMA-HdB) weight reduction was observed in both samples for the negative control set after 21 days. In contrast, the weight of poly DMAEMA-OB and poly DMAEMA-HdB showed higher reduction by 75.5% and 44.2% respectively, due to the presence of enzymes.

The poly DMAEMA-OB degraded more quickly than the poly DMAEMA-HdB (C16) due to its shorter hydrocarbon chain of eight carbon chains. Compared to the longer chains, shorter hydrocarbon chains show lessened van der Waals force. As a result, polymers with shorter hydrocarbon chains degrade more rapidly than those with longer chains, since a shorter chain corresponds to a higher hydrophilic content, which accelerates breakdown (Slor et al. 2021).

In the DMAEMA backbone of this amphiphilic polymer structure, lipase enzymes are utilized to break bonds on the ester groups (Bixenmann, Stickdorn & Nuhn 2020; Kupczak, Mielanczyk & Neugebauer 2021a). As anticipated, samples bearing lipase enzymes on the ester linkages in these two amphiphilic polymers showed faster rates of breakdown than the negative control setup (Acik 2020). The splitting of these polymers is expected to release hydroxy acids, which elevate the number of amine groups in the DMAEMA main chain, further creating electrostatic repulsion and boosting interactions with water molecules (Kupczak, Mielanczyk & Neugebauer 2021a). This condition reduces the weight of the polymer sample. These findings highlight that hydrocarbon chain length plays a pivotal role in dictating polymer degradability, as variations in chain length modulate the amphiphilic nature of the structure, thereby governing its susceptibility to enzymatic degradation pathways.

The next analysis is the determination of functional groups to ensure that the degradation process actually occurs. The lipase enzyme will break the chain of the ester group in the DMAEMA main chain, producing carboxylic acid and alcohol (Chandra et al. 2020). However, only the poly/DMAEMA-HdB sample can be analyzed by the ATR FTIR tool because it is still in solid form after drying. Meanwhile, poly/DMAEMA-OB samples easily melt at room temperature, even after being removed from the dryer cabinet. Analysis has been carried out for poly/DMAEMA-OB samples, but no results can be obtained. The ATR FTIR device concept only reflects infrared (IR) light from materials with a high refractive index (Liu & Kazarian 2022).

Figure 4 shows the FTIR spectral results for poly/DMAEMA-HdB samples before degradation and after degradation on days 5, 13, 18, and 21. It should be noted that the FTIR analysis in this study is used as a qualitative tool to identify functional group changes during degradation; no quantitative peak deconvolution or intensity ratio analysis was performed. In the results, no new absorption peaks were observed. This is because the degradation results are expected to produce carboxylic acid and alcohol compounds, which have functional groups -OH, C=O, and C-O-H, which are the same functional groups as the original amphiphilic polymers. As a result, degradation appears as changes in peak intensity, position, and band shape. Since no significant differences or relative decreases were found in the degradation curve with respect to the non-degradation curve, it is hypothesized that the degradation does not occur as a whole in the amorphous and crystalline regions (Rosato et al. 2022).

Wide absorption peaks indicate -OH strain can be observed in the range of 3393 - 3395 $cm^{-1,}$ Next, the spectrum of the carbonyl group stretch -C=O is observed in the range of 1721 - 1723 cm^{-1} with sharp peaks. While the -C–O stretch was in the range of 1234 cm^{-1}, with slight displacement compared to the sample before degradation, which was at 1266 cm^{-1}. The backbone of DMAEMA partial ester bond cleavage is compatible with these slight spectrum shifts, but there was no indication of C–N bond breakage. Significantly, the increasing physical degradation observed in SEM analysis, observed as polymer chain scission, reduced structural integrity, and surface erosion, corresponds with these FTIR-detected chemical changes.

All spectra show a sharp peak at 2852 - 2926 $cm^{-1,}$ displaying the C–H stretch vibrations of the methyl $-CH_{2-}$ group. However, the changing shape of the peak can be observed on the 18th and 21st days. The decrease in the C–H stretching bands (≈2850-2950 $cm^{-1)}$ with increasing incubation time suggests changes in the aliphatic components of the polymer during enzymatic exposure.

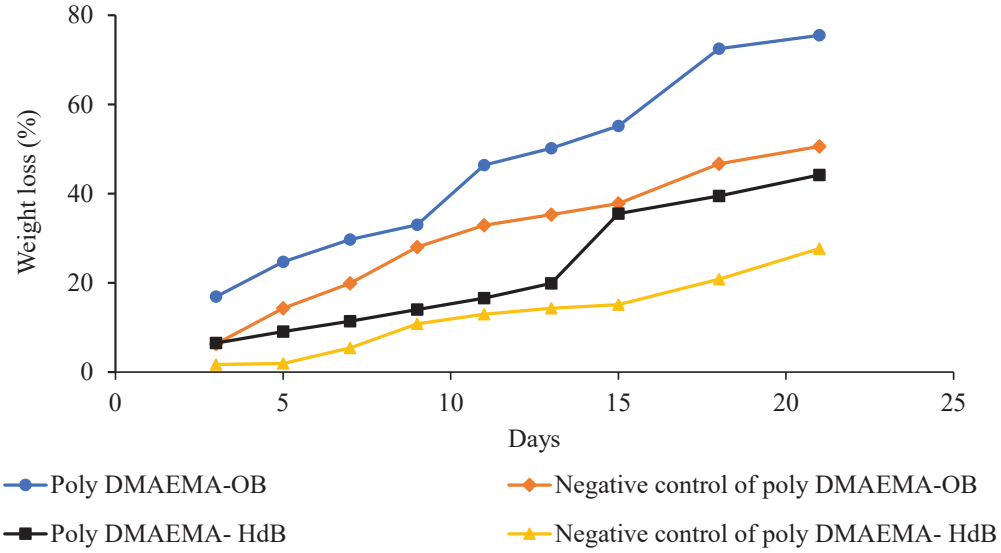

FIGURE 3. Weight loss rate in the enzymatic hydrolysis decomposition test of poly DMAEMA-OB and poly DMAEMA-HdB samples in PBS solution for 21 days

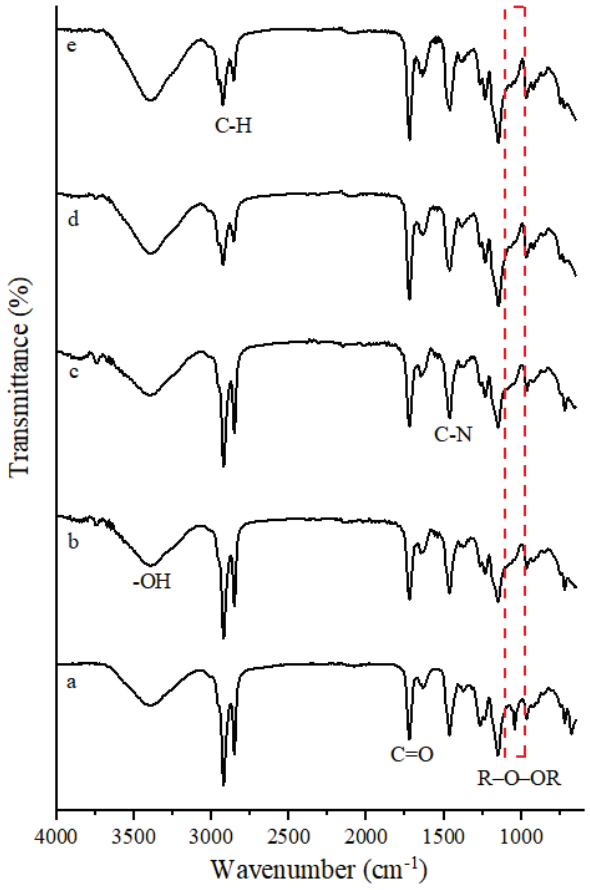

FIGURE 4. FTIR spectrum for enzymatic hydrolysis test of samples (a) poly DMAEMA-HdB before decomposition, (b) poly DMAEMA-HdB after 5 days of decomposition, (c) poly DMAEMA-HdB after 13 days of decomposition, (d) poly DMAEMA-HdB after 18 days of decomposition, and (e) poly DMAEMA-HdB after 21 days of decomposition. The red box highlighted the degradation of the peroxide band at 1043 cm^{-1}

Samples	Magnification 200×; 500×	Magnification 1000×
a)	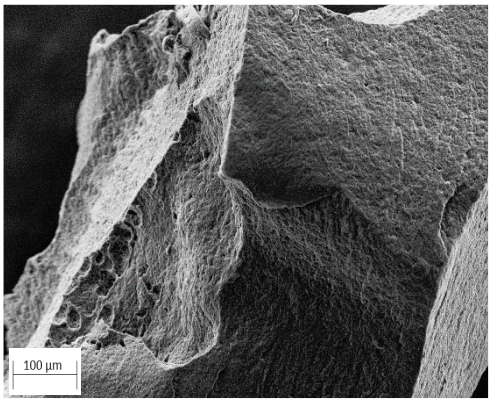	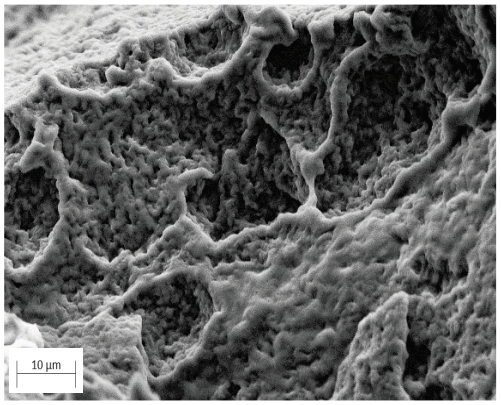
b)	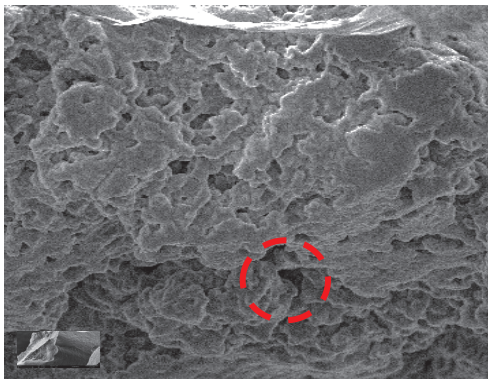	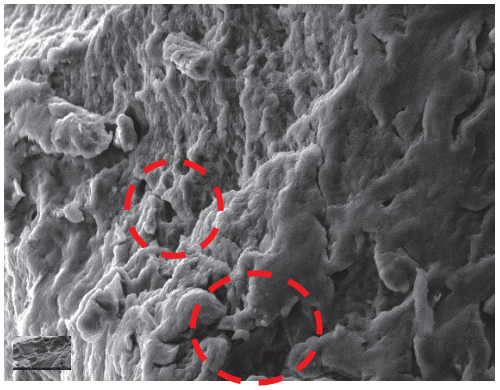
c)	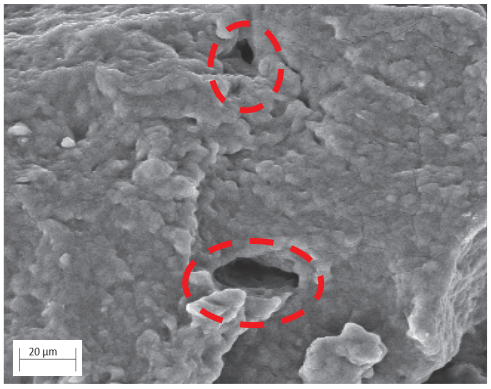	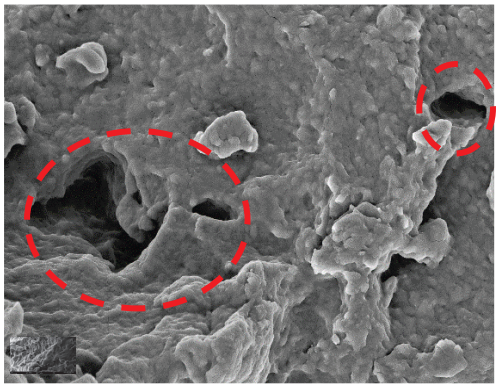
d)	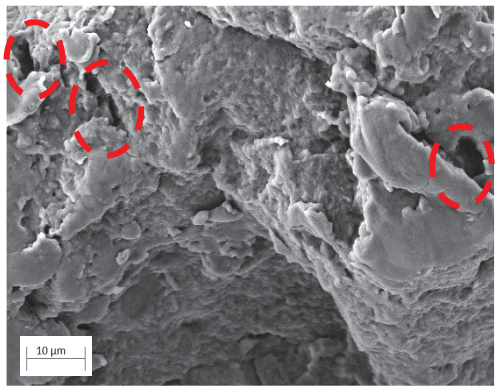	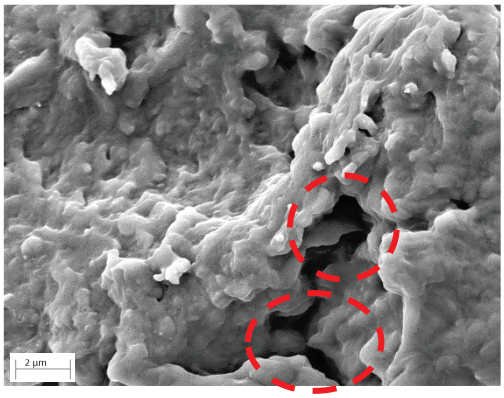

e)

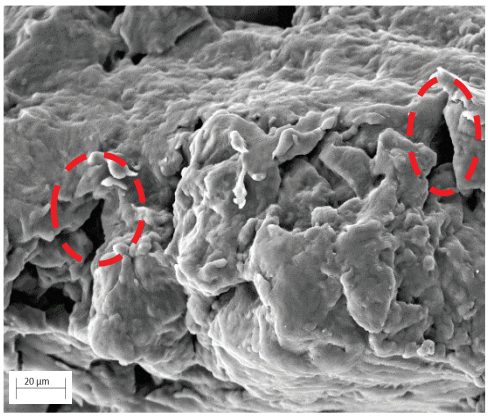

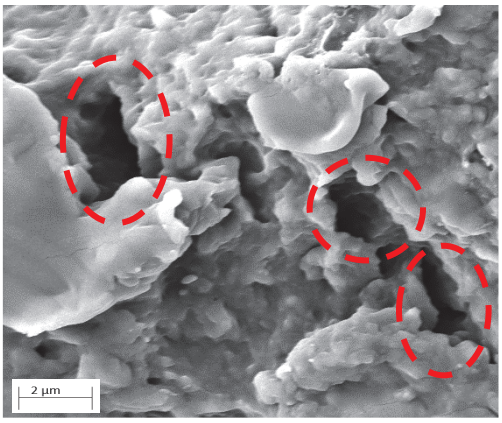

f)

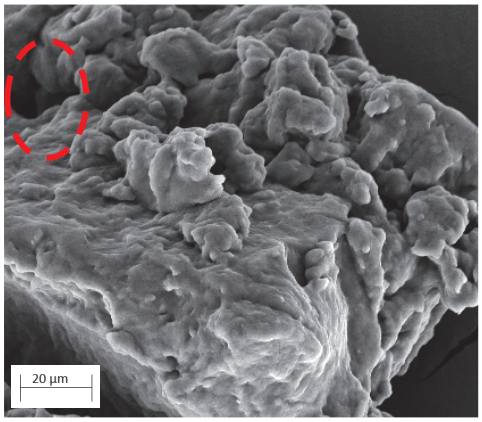

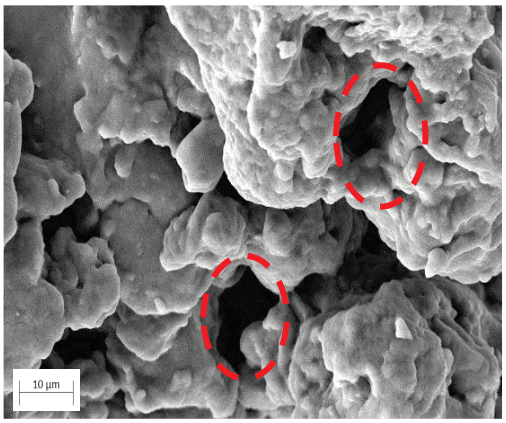

g)

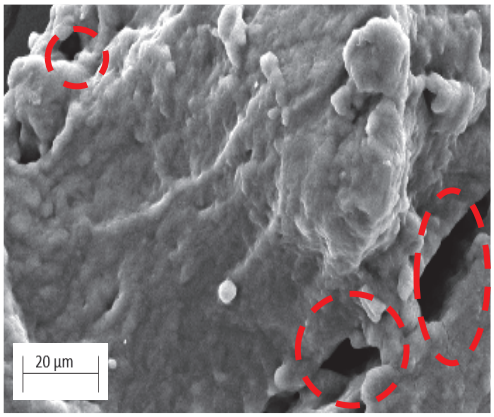

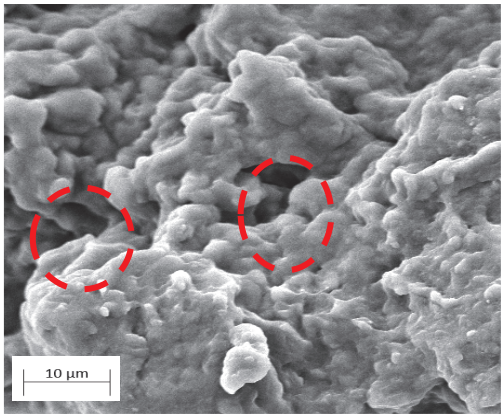

h)

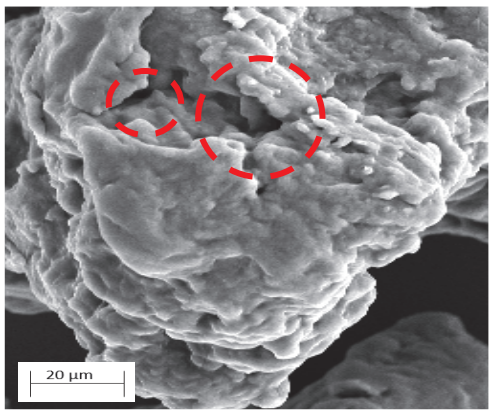

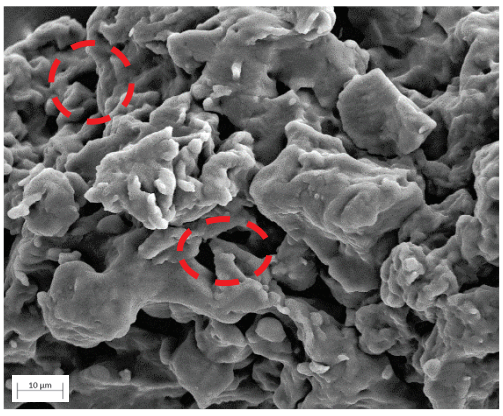

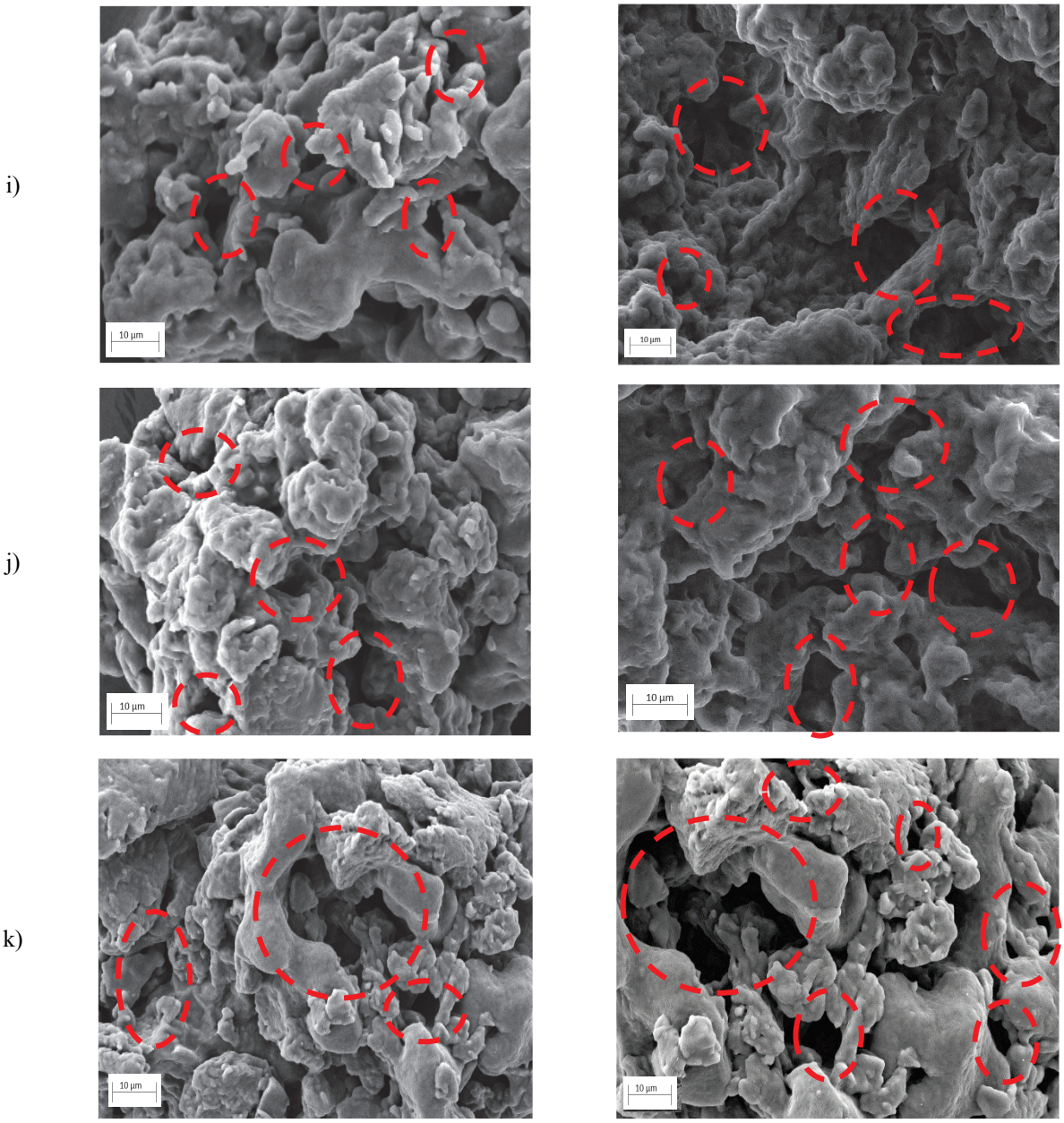

FIGURE 5. SEM micrograph of (a) poly DMAEMA-HdB sample before decomposition, and (b) poly DMAEMA-HdB sample in enzyme-free PBS solution (negative control) and poly DMAEMA-HdB sample in PBS solution with the presence of lipase enzyme for (c) day 3; (d) day 5; (e) day 7; (f) day 9; (g) day 11; (h) day 13; (i) day 15; (j) day 18, and (k) day 21

While enzymes do not directly cleave C–H bonds, polymer chain scission and structural modification during degradation can result in a reduced contribution from CH-containing segments, leading to lower FTIR peak intensities. This trend reflects the time-dependent progression of enzymatic degradation. A recent study by Kang et al. (2026) explained that this happened due to the reduced surface of hydrophobicity upon immobilization, and it reflected how lipase catalyzes ester bond hydrolysis on the hydrophobic surface of the polymer. The band at 1635 - 1649 cm^{-1} shows the C=C peak range on the DMAEMA main chain in this polymer.

Significant C – N stretching with sharp peaks was still visible on all polymer samples until the 21st day of degradation. The range of these bands is at 1461 - 1463 cm^{-1} and 1149 cm^{-1}. This proves that there is no C – N bonding done by the lipase enzyme. Notably, the absorption band at 1043 cm^{-1}, attributed to peroxide-related

bonds (Chen et al. 2007), was present in the non-degraded sample but absent in all degraded samples. Unlike minor peak shifts, the disappearance of this band provides clear qualitative evidence of chemical modification during enzymatic degradation. Confirmation of this degradation can be observed in the subsequent analysis, which is the observation of the morphology of the polymer surface using SEM.

SEM analysis was carried out to see the pore formation, damage and defects that occurred on the surface of the sample after undergoing a degradation test. This analysis was also carried out only on poly DMAEMA-HdB samples, as highly hygroscopic poly DMAEMA-OB samples were a limitation in this analysis. Figure 5 shows the SEM micrographs over the poly DMAEMA-HdB sample before decomposition (200× and 1000× magnifications); negative control flasks, i.e., poly DMAEMA-HdB samples in PBS solution for 5 days without the presence of enzymes (200× and 1000× magnification) and poly DMAEMA-HdB samples in PBS solution for 21 days (500× and 1000× magnifications) in the presence of lipase enzymes.

Based on morphological analysis, there were significant changes between the samples before and after degradation. The surface of the sample before degradation appears smooth and clean, with a solid-looking polymer wall structure. The sample also has no visible pores on its surface. The morphology of the sample in the negative control shows a slightly rough surface with little pore formation (red circles). Polymer wall structures also look quite dense with minimal damage. This supports the results of the percentage weight loss of the sample, where the negative control also shows that the degradation process occurs even in the absence of enzymes. The poly DMAEMA-HdB originally had hydrophilic characteristics, so in this case, it easily attracts the -OH group (Kalita et al. 2020) in the PBS solution. As a result, the hydrolysis process occurs, and this leads to the formation of pores and damage to the polymer surface.

Meanwhile, for samples subjected to enzymatic degradation tests, pore formation, holes, cracks, erosion marks and roughness on the polymer surface (Chaudhary & Vijayakumar 2020) were very noticeable, indicating an attack on the polymer. The longer the test day, the worse the damage became. These SEM analysis findings correlate with FTIR results showing that the polymer matrix gradually weakened as a result of ester bond breaking and functional group modification. Severe chain scission and localized collapse of polymer domains are further indicated by large surface cracks and enlarged pore structures seen after prolonged enzymatic exposure (18-21 days). Pore formation on polymer surfaces during enzymatic hydrolysis was also reported by Wei's (Wei et al. 2022) which correlates with heterogeneous hydrolysis rates across polymer surfaces, i.e., amorphous-crystalline structure of polymers, wide molecular weight distribution, and the presence of defects (gas bubbles)/fillers/additives in the sample.

On days three through seven, the wall structure appears rather compact; however, from days nine through twenty-one, it seems to be getting more damaged and deteriorated. These results are consistent with the observed trend of increasing weight loss percentage as the degradation time extends (Kupczak, Mielanczyk & Neugebauer 2021a). In another report led by Kupczak, Mielanczyk and Neugebauer (2021b), they mentioned that the presence of an ester bond in the poly DMAEMA main chain resulted in an increase in degradation rate via enzymatic degradation.

THERMAL DEGRADATION TEST

Figure 6 depicts thermogravimetric analysis (TGA) thermograms and derivative weight (DTG) curves for amphiphilic polymers in the environment. Both polymers had good thermal stability at lower temperatures; however, poly DMAEMA-HdB began to degrade at approximately 188 °C, whilst poly DMAEMA-OB remained stable up to nearly 200 °C. Weight loss below these temperatures is caused by the elimination of adsorbed moisture, residual solvents, or low-molecular-weight volatiles, which is followed by the major degradation process at higher temperatures (Guo et al. 2021; Mousavi et al. 2024; Neelamegan et al. 2020). Table 1 summarizes the findings for the onset degradation temperature ($T_{onset,}$ first degradation (T_1), second degradation (T_2), third degradation (T_3), weight loss, and residual weight at 600 °C.

Poly DMAEMA-OB-5h was found to exhibit the highest molecular weight among the synthesized polymers. Despite having the longest side chain moieties, poly DMAEMA-HdB-5h showed a comparatively lower molecular weight, which contributed to its reduced thermal stability. This observation is consistent with the general principle of polymers in which lower molecular weights are more susceptible to degradation, as they possess fewer chain entanglements, thereby requiring less energy to initiate chain scission. As a result, poly DMAEMA-OB exhibits a higher char residue with 2.5% residual mass as compared to poly DMAEMA-HdB (1.5% residual mass) due to its higher molecular weight and shorter side-chain moieties, which enhance structural rigidity and promote char stability. Overall, the thermal stability of polymeric systems is strongly governed by both molecular weight and chemical structure (Park et al. 2021).

The onset of thermal degradation (T_{onset}) for poly DMAEMA-HdB-5h was observed at 188 °C, indicating the initial decomposition of the polymer prior to the first major degradation event. Poly DMAEMA-HdB-5h presented three stages of thermal breakdown profile. The first degradation stage, which occurs at 236 °C, is attributed to the loss of the $-OCH_2CH_2N(CH_3)_2$ group fragments. The second degradation stage is observed at 317 °C, corresponding to the elimination of the $-OCH_2CH_2N^+(CH_3)_2(C_{16}H_{33})$ Br^- group (Kong et al. 2016). Meanwhile, the third degradation stage appears at 415 °C, within the region

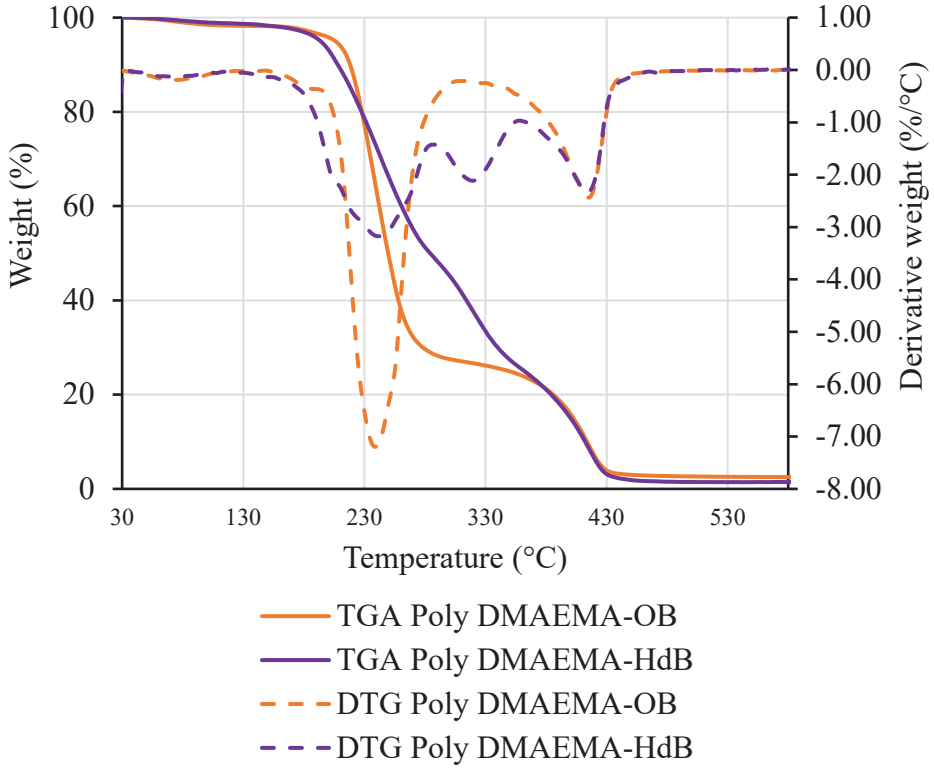

FIGURE 6. TGA thermograms and DTG curves of amphiphilic polymers

TABLE 1. Data of thermogravimetric analysis for poly DMAEMA-HdB-5h and poly DMAEMA-OB-5h

Polymer	Onset degradation, T_{onset} (°C)	First degradation, T_1 (°C)	Weight loss (%)	Second degradation, T_2 (°C)	Weight loss (%)	Third degradation, T_3 (°C)	Weight loss (%)	Residual mass (%)
DMAEMA-HdB	188	236	49.5	317	23.7	415	24.1	1.5
DMAEMA-OB	204	239	71.0	415	24.7	-	-	2.5

of significant polymer weight loss (400-500 °C) caused by the degradation of the polymer main chain involving the DMAEMA units (Soykan & Tüfekçi 2025). In contrast, poly DMAEMA-OB-5h exhibited higher thermal stability, with the onset of thermal degradation (T_{onset}) observed at approximately 204 °C, which is higher than that of poly DMAEMA-HdB-5h. The TGA profile showed a two-stage thermal degradation behavior, with major degradation events occurring at around 239 °C and 415 °C, respectively. These shifts to higher degradation temperatures highlight the greater stability of poly DMAEMA-OB-5h compared to poly DMAEMA-HdB-5h, which can be attributed to its higher molecular weight and shorter side-chain moieties that enhance resistance to thermal scission (Omer et al. 2021).

The dissociation of quaternary amine groups from the polymer occurred at 230 °C (Dalhatu et al. 2021; Mathew et al. 2018), that is the smaller part of the polymer (Abdelaziz et al. 2021; Cazotti et al. 2020). The results of Tarmizi et al. (2023), who used TGA/FTIR equipment to segment the O-H and N-H groups, concur with this. The results of this investigation addressing the thermal behavior of the backbone of DMAEMA were in great agreement with the literature describing the breakdown of the final stage, which was connected to the backbone of DMAEMA polymers, at temperatures above 400 °C (Bomfim et al. 2009; Okten, Canakci & Orakdogen 2019).

CONCLUSION

Amphiphilic DMAEMA-based polymers were successfully synthesized and characterized, demonstrating that alkyl chain length introduced during bromoalkene quaternization plays a critical role in emphasizing amphiphilicity and, hence, degradation behavior under thermal and enzymatic conditions. Poly DMAEMA-

OB-5h, with shorter alkyl chains but a higher molecular weight, has a better-balanced amphiphilic structure with improved hydrophilicity, allowing for greater water penetration and enzyme accessibility. This resulted in faster lipase-assisted hydrolysis and higher heat stability compared to poly DMAEMA-HdB-5h. Meanwhile, the longer alkyl chains in poly DMAEMA-HdB-5h improved hydrophobic interactions and chain packing, resulting in better structural rigidity, lower thermal resistance, and reduced enzymatic degradability. Enzymatic degradation was validated by ester bond cleavage within the DMAEMA backbone, whereas SEM and FTIR investigations showed surface erosion and chemical alteration during hydrolysis. Indeed, these findings show a distinct link between structure, amphiphilicity, and degradation, suggesting that poly DMAEMA-OB-5h is ideal for applications requiring more biodegradability and environmental adaptability. In comparison, poly DMAEMA-HdB-5h is superior for applications that require more controlled degradation and thermal stability, particularly in functional and biomedical material systems.

ACKNOWLEDGMENTS

We would like to thank the Department of Chemical Sciences and Department of Biological Sciences and Biotechnology, Faculty of Science and Technology; the Center of Diagnostics, Therapeutics & Investigations, Faculty of Health Sciences, Universiti Kebangsaan Malaysia, and the Malaysian Nuclear Agency. The research project was financed by Universiti Kebangsaan Malaysia by the Dana Cabaran Perdana grant (Code: DCP-2017-003/1).

REFERENCES

Abdelaziz, A.I.E., Elsaeed, S.M., Zaki, E.G., Aboaly, M.M., Abdel-Raouf, M.E.S. & Al-Sabagh, A.M. 2021. Preparation and characterization of a new family of bio-interpenetrating network hydrogel based on a green method. *Egyptian Journal of Chemistry* 64(12): 7451-7464.

Acik, G. 2020. Preparation of antimicrobial and biodegradable hybrid soybean oil and poly (L -lactide) based polymer with quaternized ammonium salt. *Polymer Degradation and Stability* 181: 109317.

Aina Aqila Arman Alim, Siti Salwa Mohammad Shirajuddin & Farah Hannan Anuar. 2022. A review of nonbiodegradable and biodegradable composites for food packaging application. *Journal of Chemistry* 2022: Article ID. 7670819.

Aina Aqila Arman Alim, Azizah Baharum, Siti Salwa Mohammad Shirajuddin & Farah Hannan Anuar. 2023. Blending of low-density polyethylene and poly(butylene succinate) (LDPE/PBS) with polyethylene–graft–maleic anhydride (PE–g–MA) as a compatibilizer on the phase morphology, mechanical and thermal properties. *Polymers* 15(2): 261.

Albayati, S.H., Masomian, M., Ishak, S.N.H., Ali, M.S.B.M., Thean, A.L., Shariff, F.B.M., Noor, N.D.B.M. & Rahman, R.N.Z.R.A. 2020. Main structural targets for engineering lipase substrate specificity. *Catalysts* 10(7): 747.

Ali, M., Garg, A., Srivastava, A. & Arora, P.K. 2025. The role of antimicrobial peptides in overcoming antibiotic resistance. *Microbe (Netherlands)* 7: 100337.

Bednarz, S., Błaszczyk, A., Błazejewska, D. & Bogdał, D. 2014. Free-radical polymerization of itaconic acid in the presence of choline salts: Mechanism of persulfate decomposition. *Catalysis Today* 257: 297-304.

Bixenmann, L., Stickdorn, J. & Nuhn, L. 2020. Amphiphilic poly(esteracetal)s as dual pH-and enzyme-responsive micellar immunodrug delivery systems. *Polymer Chemistry* 11(13): 2441-2456.

Bomfim, J.A.S., Mincheva, R., Beigbeder, A., Persenaire, O. & Dubois, P. 2009. (Quaternized/betainized) amino-based amphiphilic block copolymers: Quantitative composition characterization via FTIR and thermogravimetry. *E-Polymers* 9(1): 035.

Casanova, M., Olleik, H., Hdiouech, S., Roblin, C., Cavalier, J.F., Point, V., Jeannot, K., Caron, B., Perrier, J., Charriau, S., Lafond, M., Guillaneuf, Y., Canaan, S., Lefay, C. & Maresca, M. 2023. Evaluation of the efficiency of random and diblock methacrylate-based amphiphilic cationic polymers against major bacterial pathogens associated with cystic fibrosis. *Antibiotics* 12(1): 120.

Cazotti, J.C., Fritz, A.T., Garcia-Valdez, O., Smeets, N.M.B., Dubé, M.A. & Cunningham, M.F. 2020. Graft modification of starch nanoparticles with pH-responsive polymers via nitroxide-mediated polymerization. *Journal of Polymer Science* 58(16): 2211-2220.

Chandra, P., Enespa, Singh, R. & Arora, P.K. 2020. Microbial lipases and their industrial applications: A comprehensive review. *Microbial Cell Factories* 19(1): 169.

Chaudhary, A.K. & Vijayakumar, R.P. 2020. Studies on biological degradation of polystyrene by pure fungal cultures. *Environment, Development and Sustainability* 22(5): 4495-4508.

Chen, J., Wu, Z., Yang, L., Zhang, Q., Sun, J., Shi, Y., Xia, L. & Kaetsu, I. 2007. Grafting copolymerization of N,N-dimethyacrylaminoethylmethacrylate (DMAEMA) onto preirradiated polypropylene films. *Radiation Physics and Chemistry* 76(8-9): 1367-1370.

Cook-Chennault, K., Anaokar, S., Medina Vázquez, A.M. & Chennault, M. 2024. Influence of high strain dynamic loading on HEMA–DMAEMA hydrogel storage modulus and time dependence. *Polymers* 16(13): 1797.

Dalhatu, S.N., Modu, K.A., Mahmoud, A.A., Adamu, H.M. & Murtala, R. 2021. Ultrasonic assisted synthesis and characterization of chitosan graf with 2- (dimethylaminoethylmethacrylate) (DMAEMA) Cs-G-PDMAEMA. *Journal of Physical Sciences* 3(1): 1-10.

Danielsen, S.P.O., Beech, H.K., Wang, S., El-Zaatari, B.M., Wang, X., Sapir, L., Ouchi, T., Wang, Z., Johnson, P.N., Hu, Y., Lundberg, D.J., Stoychev, G., Craig, S.L., Johnson, J.A., Kalow, J.A., Olsen, B.D. & Rubinstein, M. 2021. Molecular characterization of polymer networks. *Chemical Reviews* 121(8): 5042-5092.

Fu, X., Zhang, Y., Jia, X., Wang, Y. & Chen, T. 2022. Research progress on typical quaternary ammonium salt polymers. *Molecules* 27(4): 1267.

Gaytán, I., Burelo, M. & Loza-Tavera, H. 2021. Current status on the biodegradability of acrylic polymers: Microorganisms, enzymes and metabolic pathways involved. *Applied Microbiology and Biotechnology* 105(3): 991-1006.

Guo, H., Ma, L., Yan, C. & Ma, X. 2021. A study on the preparation of polycation gel polymer electrolyte for supercapacitors. *RSC Advances* 11(40): 24995-25003.

Im, D., Gavande, V., Lee, H.Y. & Lee, W.K. 2023. Influence of molecular weight on the enzymatic degradation of PLA isomer blends by a Langmuir system. *Materials* 16(14): 5087.

Kalita, N.K., Bhasney, S.M., Kalamdhad, A. & Katiyar, V. 2020. Biodegradable kinetics and behavior of bio-based polyblends under simulated aerobic composting conditions. *Journal of Environmental Management* 261: 110211.

Kang, Y., Zhang, Z., Li, S., Wang, C., Chang, T., Hao, Y. & Liu, J. 2026. Engineered alkyl-chain functionalized hyper-crosslinked polymers as robust lipase hosts for synthesis fatty esters in aqueous solution. *Fuel* 405: 136769.

Kong, D.C., Yang, M.H., Zhang, X.S., Du, Z.C., Fu, Q., Gao, X.Q. & Gong, J.W. 2021. Control of polymer properties by entanglement: A review. *Macromolecular Materials and Engineering* 306(12): 2100536.

Kong, Z., Wu, X., Wei, J., Zhang, H. & Cui, L. 2016. Preparation and characterization of hydrophilicity fibers based on 2-(dimethylamino)ethyl methacrylate grafted polypropylene by UV- irradiation for removal of Cr(VI) and as(V). *Journal of Polymer Research* 23: 1-9.

Koufakis, E., Manouras, T., Anastasiadis, S.H. & Vamvakaki, M. 2020. Film properties and antimicrobial efficacy of quaternized PDMAEMA brushes: Short vs long alkyl chain length. *Langmuir* 36(13): 3482-3493.

Koutsougera, M.F., Adamopoulou, S., Druvari, D., Vlamis-Gardikas, A., Iatridi, Z. & Bokias, G. 2025. Multifunctional amphiphilic biocidal copolymers based on N-(3-(Dimethylamino)propyl) methacrylamide Exhibiting pH-, thermo-, and CO_2-sensitivity. *Polymers* 17(14): 1896.

Kupczak, M., Mielanczyk, A. & Neugebauer, D. 2021a. The influence of polymer composition on the hydrolytic and enzymatic degradation of polyesters and their block copolymers with PDMAEMA. *Materials* 14(13): 3636.

Kupczak, M., Mielańczyk, A. & Neugebauer, D. 2021b. PDMAEMA/polyester miktopolymers: Synthesis via in-out approach, physicochemical characterization and enzymatic degradation. *Materials* 14(5): 1277.

Leggieri, M.R.T., Kaldéus, T., Johansson, M. & Malmström, E. 2023. PDMAEMA from α to ω chain ends: Tools for elucidating the structure of poly(2-(dimethylamino)ethyl methacrylate). *Polymer Chemistry* 14(11): 1241-1253.

Li, M., Jin, E., Qiao, Z. & Zhao, R. 2018. Effects of alkyl chain length of aliphatic dicarboxylic ester on degradation properties of aliphatic-aromatic water-soluble copolyesters for warp sizing. *Fibers and Polymers* 19(3): 538-547.

Liu, G.L. & Kazarian, S.G. 2022. Recent advances and applications to cultural heritage using ATR-FTIR spectroscopy and ATR-FTIR spectroscopic imaging. *Analyst* 147(9): 1777-1797.

Lu, G., Wu, D. & Fu, R. 2007. Studies on the synthesis and antibacterial activities of polymeric quaternary ammonium salts from dimethylaminoethyl methacrylate. *Reactive and Functional Polymers* 67(4): 355-366.

Luo, X., Ye, X., Ding, L., Zhu, W., Yi, P., Zhao, Z., Gao, H., Shu, Z., Li, S., Sang, M., Wang, J., Zhong, W. & Chen, Z. 2021. Fine-tuning of alkaline residues on the hydrophilic face provides a non-toxic cationic α-helical antimicrobial peptide against antibiotic-resistant ESKAPE pathogens. *Frontiers in Microbiology* 12: 684591.

Manouras, T., Platania, V., Georgopoulou, A., Chatzinikolaidou, M. & Vamvakaki, M. 2021. Responsive quaternized PDMAEMA copolymers with antimicrobial action. *Polymers* 13(18): 3051.

Mathew, M.E., Ahmad, I., Thomas, S., Daik, R. & Kassim, M. 2018. Synthesis and characterization of poly (benzyl trimethyl ammonium chloride) ionic polymer. *AIP Conference Proceedings*. p. 1940.

Mousavi, S.M., Babazadeh, M., Nemati, M., Es'haghi, M. & Babazadeh, M. 2024. Fabrication of graphene oxide nanocomposite based on poly(3-hydroxybutyrate)-chitosan as a useful drug carrier. *Karaj Branch Journal of Applied Chemical Research* 18(1): 41-59.

Mushtaq, S., Ahmad, N.M., Mahmood, A. & Iqbal, M. 2021. Antibacterial amphiphilic copolymers of dimethylamino ethyl methacrylate and methyl methacrylate to control biofilm adhesion for antifouling applications. *Polymers* 13(2): 216.

Neelamegan, H., Yang, D.K., Lee, G.J., Anandan, S., Sorrentino, A. & Wu, J.J. 2020. Synthesis of magnetite-based polymers as mercury and anion sensors using single electron transfer-living radical polymerization. *ACS Omega* 5(13): 7201-7210.

Okten, N.S., Canakci, C.C. & Orakdogen, N. 2019. Hertzian elasticity and triggered swelling kinetics of poly(amino ester)-based gel beads with controlled hydrophilicity and functionality: A mild and convenient synthesis via dropwise freezing into cryogenic liquid. *European Polymer Journal* 114(February): 176-188.

Omer, A.M., Tamer, T.M., Khalifa, R.E., Eltaweil, A.S., Agwa, M.M., Sabra, S., Abd-Elmonem, M.S., Mohy-Eldin, M.S. & Ziora, Z.M. 2021. Formulation and antibacterial activity evaluation of quaternized aminochitosan membrane for wound dressing applications. *Polymers* 13(15): 2428.

Park, S., Thanakkasaranee, S., Shin, H., Lee, Y., Tak, G. & Seo, J. 2021. PET/bio-based terpolyester blends with high dimensional thermal stability. *Polymers* 13(5): 728.

Rahman, M.S., Brown, J., Murphy, R., Carnes, S., Carey, B., Averick, S., Konkolewicz, D. & Page, R.C. 2021. Polymer modification of lipases, substrate interactions, and potential inhibition. *Biomacromolecules* 22(2): 309-318.

Rauschkolb, J.C., Ribeiro, B.C., Feiden, T., Fischer, B., Weschenfelder, T.A., Cansian, R.L. & Junges, A. 2022. Parameter estimation of Mark-Houwink equation of polyethylene glycol (PEG) using molecular mass and intrinsic viscosity in water. *Biointerface Research in Applied Chemistry* 12(2): 1778-1790.

Ren, N., Yu, C. & Zhu, X. 2021. Topological effect on macromonomer polymerization. *Macromolecules* 54(13): 6101-6108.

Rodríguez-Contreras, A., Calafell-Monfort, M. & Marqués-Calvo, M.S. 2012. Enzymatic degradation of poly(3-hydroxybutyrate-co-4-hydroxybutyrate) by commercial lipases. *Polymer Degradation and Stability* 97(4): 597-604.

Rosato, A., Romano, A., Totaro, G., Celli, A., Fava, F., Zanaroli, G. & Sisti, L. 2022. Enzymatic degradation of the most common aliphatic bio-polyesters and evaluation of the mechanisms involved: An extended study. *Polymers* 14(9): 1850.

Santoro, O. & Izzo, L. 2024. Antimicrobial polymer surfaces containing Quaternary Ammonium Centers (QACs): Synthesis and mechanism of action. *International Journal of Molecular Sciences* 25(14): 7587.

Slor, G., Olea, A.R., Pujals, S., Tigrine, A., De La Rosa, V.R., Hoogenboom, R., Albertazzi, L. & Amir, R.J. 2021. Judging enzyme-responsive micelles by their covers: Direct comparison of dendritic amphiphiles with different hydrophilic blocks. *Biomacromolecules* 22(3): 1197-1210.

Soykan, C. & Tüfekçi, B. 2025. Antibacterial amphiphilic composites of poly(diethylaminoethyl methacrylate-co-ethyl methacrylate)/polyindole controlling biofilm adhesion for antifouling investigations. *El-Cezeri Journal of Science and Engineering* 12(2): 167-175.

Stawski, D. 2023. Poly(N,N-dimethylaminoethyl methacrylate) as a bioactive polyelectrolyte - production and properties. *Royal Society Open Science* 10(9): 230188.

Tarmizi, Z.I.A., Ali, R.R., Nasef, M.M., Radzi, A.M.M., Akim, A.M., Eshak, Z., Noor, S.M., Shafie, N.F.A. & Faizo, S.M. 2023. Thermal and degradation analysis of electrospun polyurethane prepared using radiation induced grafting. *Journal of Advanced Research in Fluid Mechanics and Thermal Sciences* 108(2): 110-121.

Wei, X.F., Capezza, A.J., Cui, Y., Li, L., Hakonen, A., Liu, B. & Hedenqvist, M.S. 2022. Millions of microplastics released from a biodegradable polymer during biodegradation/enzymatic hydrolysis. *Water Research* 211: 118068.

Zografos, A., Lynd, N.A., Bates, F.S. & Hillmyer, M.A. 2021. Impact of macromonomer molar mass and feed composition on branch distributions in model graft copolymerizations. *ACS Macro Letters* 10(12): 1622-1628.

*Corresponding author; email: rusli.daik@ukm.edu.my